IEEE Access
Multidisciplinary | Rapid Review | Open Access Journal

Received May 14, 2019, accepted May 30, 2019, date of publication June 6, 2019, date of current version June 26, 2019.

Digital Object Identifier 10.1109/ACCESS.2019.2921340

The Folded Normal Distribution: A New Model for the Small-Scale Fading in Line-of-Sight (LOS) Condition

JUAN REIG[1], (Senior Member, IEEE), VICENT MIQUEL RODRIGO PEÑARROCHA[1], LORENZO RUBIO[1], (Senior Member, IEEE), MARÍA TERESA MARTÍNEZ-INGLÉS[2], AND JOSE MARÍA MOLINA-GARCÍA-PARDO[3]

[1]Electromagnetic Radiation Group, Universitat Politècnica de València, 46022 Valencia, Spain
[2]University Center of Defense, San Javier Air Force Base, MDE, Universidad Politécnica de Cartagena, 30720 Murcia, Spain
[3]Departamento Tecnologías de la Información y las Comunicaciones, Universidad Politécnica de Cartagena, 30720 Murcia, Spain

Corresponding author: Juan Reig (jreigp@dcom.upv.es)

This work was supported by the Ministerio de Economía, Industria y Competitividad of the Spanish Government under the national projects TEC2017-86779-C2-2-R and TEC2016-78028-C3-2-P, through the Agencia Estatal de Investigación (AEI) and the Fondo Europeo de Desarrollo Regional (FEDER).

ABSTRACT In this paper, a novel form of the folded normal (FN) distribution has been proposed to model the small-scale fading in wireless communications. From a multiple-input multiple-output (MIMO) measurement campaign conducted in a lab environment with the line-of-sight (LOS) conditions at both the 60 and the 94 GHz bands, the authors obtain the parameters of the Rician, FN, and κ-μ distributions. These parameters have been calculated by using the least square (LS) approximation and with techniques of statistical inference. The FN distribution provides the best fitting to the experimental results using the Kolmogorov–Smirnov (K–S) test for the inferred estimators with values of the fulfillment of 100% and 69.82% at the 60 and 94 GHz bands, respectively, for a significance level of 1%.

INDEX TERMS 5G mobile communication, millimeter wave propagation, fading channels.

I. INTRODUCTION

The received envelope in a wireless communication channel experiments two physical effects. On the one hand, the multipath components cause rapid and deep fading in amplitude over displacements of few wavelengths. The amplitude of this fast fading or small-scale fading has been traditionally modeled using the Rayleigh [1], Rician [2], Nakagami-*m* [3] and Weibull [4] distributions. On the other hand, the received signal fluctuates slowly around a mean in displacements of hundreds of wavelengths. This variation is known as the long-term fading or shadowing due to the temporal blockage of the direct component between the transmitter and received terminal. The shadowing is commonly modeled statistically by a lognormal distribution.

Specifically, the Rician distribution faithfully models a dominant component together with a small component in-phase and quadrature Gaussian distributed, which corresponds to a situation typically found in line-of-sight (LOS) conditions.

The associate editor coordinating the review of this manuscript and approving it for publication was Ke Guan.

Nevertheless, over the last 15 years many new distributions have been proposed to model the small-scale fading in several conditions [5]–[13]. In [5], the two wave with diffuse power (TWDP) distribution was derived for the condition of two specular multipath components in the presence of other diffusely propagating waves. Furthermore, a family of distributions has been derived to model the small-scale fading in [6]–[11]. The general α-η-κ-μ model proposed by Yacoub in [6] accounts for nonlinearity of the propagation medium and multipath clustering, including the possibility of dominant components in each cluster. The α-η-κ-μ includes the α-η-μ, the α-κ-μ [7], α-μ [8], η-κ [9], κ-μ [10] and η-μ [11] as particular cases. Specifically, the κ-μ distribution describes a signal composed of clusters of multipath waves propagating in a non-homogeneous environment with a dominant component in each cluster [10]. The Rician, Rayleigh, one-sided Gaussian and Nakagami-*m* distributions are included in the κ-μ distribution for specific values of κ and μ. Recently, in [12] the κ-μ shadowed distribution has been derived to model the composite small-scale fading and shadowing. The κ-μ

shadowed distribution includes the κ-μ and η-μ distributions as particular cases [13] in a mathematically tractable model. Some of these distributions have been recently applied to model new propagation scenarios [14], [15]. In [14] the κ-μ and α-μ fading channels have been used to characterize the small-scale variations of the fading signal under LOS in different millimeter wave (mmWave) bands. Furthermore, in [15] the TWDP distribution has been proven to be more favorable than the commonly used the Rician fading model for the vehicle-to-vehicle (V2V) link in an overtaking situation with LOS condition at the 60 GHz band.

Over the last few years, intense efforts are being made to explore new frequency bands beyond 6 GHz, in particular the mmWave bands, for deploying 5G systems [16]–[19]. High capacity 5G networks require spectrum availability along with massive multiple-input multiple-output (MIMO) at the transmitter and receiver.

On the one hand, inside the V band (40-75 GHz), the 60 GHz band has been proposed for Wireless Gigabit Ethernet following the standard IEEE 802.3c [20]. In order to contribute to the better understanding of the narrowband characterization at the 60 GHz band, several small-scale analyses have been performed from measurement campaigns [21]–[24]. In [21], the received amplitude in LOS measurements carried out in three corridors of an office block with a bandwidth (BW) of 1 GHz was modeled as a Rician distribution. Using two antenna types, an open-ended waveguide (OWG) and lens, values of the mean and the standard deviation of the Rician K-factor have been calculated. In an urban environment, the small-scale amplitude has been found to follow a Rayleigh distribution with ranges up to 400 m [22]. In [23], a measurement campaign was performed in a lab environment with LOS condition. In this work, the best-fit distribution was the Rician followed by the α-μ and Nakagami-m distributions. Recently, in [24] the impact of terminal handling upon the user equipment (UE) was assessed with LOS and non-LOS (NLOS) conditions in a range of different indoor and outdoor small cell scenarios. In LOS condition, the small-scale statistic was modeled as a Rician distribution with estimated Rician K-factors ranging from 3.1 to 9.1 in a hallway, from 3.5 to 7.4 in an office, and from 4.5 to 6.9 in a car park. In NLOS condition, the small-scale distribution used was Nakagami-m with estimated fading parameters, m, varying from 2.12 to 3.77 in a hallway, from 2.27 to 3.89 in an office, and from 2.46 to 4.68 in a car park.

On the other hand, inside the W band (75-110 GHz), several analyses have been carried out at the 94 GHz band in [25], [26], mainly concentrated on modeling the propagation losses and shadowing in indoor environments. Recently, in [27] the analysis of the power delay profiles, root mean square (r.m.s.) delay spreads and specular power ratio has been performed in an indoor environment at the 94 GHz band. Small-scale amplitude distributions have been analyzed in a lab at the 94 GHz band in [28]. In this work, the best-fit distribution turned out to be the Weibull followed by the α-μ and the Rician distribution. In [29], the mean of the Rician K-factor has been evaluated as a function of the separation between transmitter (Tx) and receiver (Rx) in a lab at the 94 GHz band.

In this work, a form of the folded normal (FN) distribution is proposed to model the small-scale fading amplitude as a specific case of the κ-μ distribution. The probability density function (PDF), cumulative distribution function (CDF), moments, moment generating function and relationships with other distributions are derived in terms of the κ parameter. From MIMO measurements in an indoor lab scenario carried out at both the 60 and 94 GHz bands with LOS condition, we have calculated the parameters of the Rician, FN, and κ-μ distributions in several positions of the lab over a significant number of frequency samples, i.e., 2 048 and 1 024 frequency samples, for the 60 and 94 GHz bands, respectively. The results show that using estimators the best-fit distribution is the FN distribution among the three previous distributions.

From the results of this work, the FN distribution provides the following benefits:

1) The estimated κ parameter of the FN distribution is more stable than both the estimated Rician K-factor of the Rician distribution and the estimated κ parameter of the κ-μ distribution.
2) The FN distribution is biparametric like the Rician distribution.
3) Both the PDF and CDF of the FN distribution are simple and mathematically tractable.

The applicability of using the FN distribution to model the small-scale fading is mainly underlined for the high dependence of the performance parameters such as the average error probability and outage probability using different modulation schemes on the Rician K-factor [30]. Therefore, a more accurate estimation of this Rician K-factor through the FN distribution could contribute to a better evaluation of those performance parameters. Besides, a simpler PDF expression corresponding to the FN distribution provides less complex expressions for the average probability of error and outage probability over different modulations.

The remainder of this paper is organized as follows. In Section II, the FN distribution is derived from the κ-μ distribution and the PDF and CDF in both linear and logarithmic units are obtained in terms of the κ parameter. Section III includes the moments, the moment generating function and the relationship of the FN distribution with other distributions: Nakagami-m, Rician and κ-μ. In Section IV, a description of the MIMO measurement campaign in a lab at both the 60 and 94 GHz bands is presented. Section V presents the approximation method and the estimators used to calculate the parameters of the Rician, FN and κ-μ distributions. In Section VI, the parameters of the previous distributions are calculated and the goodness-of-fit of the analyzed distributions are compared. Finally, the conclusions are discussed in Section VII.

II. FAMILY OF κ-μ DISTRIBUTIONS

Let r be the envelope of the small-scale fading distribution calculated as

$$r = \sqrt{\sum_{i=1}^{\mu} (x_i + a_i)^2 + (y_i + b_i)^2}, \tag{1}$$

where x_i and y_i are independent Gaussian processes, with $E[x_i] = E[y_i] = 0$ and $E\left[x_i^2\right] = E\left[y_i^2\right] = \sigma^2$, being $E[\cdot]$ the expectation operator; a_i and b_i are the mean of the in-phase and quadrature multipath component i; and μ is the number of multipath components.

We can define

$$\kappa = \frac{c^2}{2\mu\sigma^2}, \tag{2}$$

where $c = \sqrt{\sum_{i=1}^{\mu}\left(a_i^2 + b_i^2\right)}$. In the next sub-sections, the PDF and CDF of the κ-μ, Rician and FN distributions will be addressed.

A. κ-μ

From [10], r follows the well-known κ-μ distribution. The PDF of r can be calculated as

$$\begin{aligned} p_r(r) = {} & \frac{2\mu(1+\kappa)^{\frac{\mu+1}{2}}}{\kappa^{\frac{\mu-1}{2}}\exp(\mu\kappa) r_m} \left(\frac{r}{r_m}\right)^{\mu} \\ & \times \exp\left(-\mu(1+\kappa)\left(\frac{r}{r_m}\right)^2\right) \\ & \times I_{\mu-1}\left(2\mu\sqrt{\kappa(1+\kappa)}\left(\frac{r}{r_m}\right)\right) \quad r \geq 0, \end{aligned} \tag{3}$$

where r_m is the r.m.s. of the distribution defined as

$$r_m = \sqrt{E\left[r^2\right]} = \sqrt{2\mu\sigma^2 + c^2}, \tag{4}$$

being $I_a(\cdot)$ the modified Bessel function of the first kind with order a [31, (8.406)]. The CDF of r is given by

$$P_r(r) = 1 - Q_{\mu}\left(\sqrt{2\mu\kappa}, \sqrt{2\mu(1+\kappa)}\left(\frac{r}{r_m}\right)\right) \quad r \geq 0, \tag{5}$$

where

$$Q_v(c,d) = \frac{1}{c^{v-1}} \int_d^{\infty} t^v \exp\left(-\frac{t^2+c^2}{2}\right) I_{v-1}(ct)\, dt \tag{6}$$

is the generalized Marcum Q function [32].

From [10], the limitation of the model given by (1) can be made less stringent by assuming μ real defined as

$$\mu = \frac{E\left[r^2\right]}{\mathrm{var}\left[r^2\right]} \frac{(1+2\kappa)}{(1+\kappa)^2}, \tag{7}$$

where $\mathrm{var}[\cdot]$ represents the variance.

If we express the envelope in logarithmic units, $\varepsilon = 20\log r = A\ln r$, where $A = 20/\ln 10$, the PDF of ε is given by

$$\begin{aligned} p_{\varepsilon}(\varepsilon) = {} & \frac{2\mu(1+\kappa)^{\frac{\mu+1}{2}}}{A\kappa^{\frac{\mu-1}{2}}\exp(\mu\kappa)} \left(\frac{\exp\left(\frac{\varepsilon}{A}\right)}{r_m}\right)^{\mu+1} \\ & \times \exp\left(-\mu(1+\kappa)\left(\frac{\exp\left(\frac{\varepsilon}{A}\right)}{r_m}\right)^2\right) \\ & \times I_{\mu-1}\left(2\mu\sqrt{\kappa(1+\kappa)}\left(\frac{\exp\left(\frac{\varepsilon}{A}\right)}{r_m}\right)\right) \\ & -\infty < \varepsilon < \infty. \end{aligned} \tag{8}$$

The CDF of ε is given by

$$\begin{aligned} P_{\varepsilon}(\varepsilon) = {} & 1 - Q_{\mu}\left(\sqrt{2\mu\kappa}, \sqrt{2\mu(1+\kappa)}\left(\frac{\exp\left(\frac{\varepsilon}{A}\right)}{r_m}\right)\right) \\ & -\infty < \varepsilon < \infty. \end{aligned} \tag{9}$$

B. RICIAN

If $\mu = 1$, r follows the Rician distribution. In this case, the κ parameter is commonly known as the Rician K-factor, which can be expressed from (2) as

$$K = \frac{c^2}{2\sigma^2}. \tag{10}$$

Substituting $\mu = 1$ in (3) and (5), the PDF and CDF of r, respectively, are given by

$$\begin{aligned} p_r(r) = {} & \frac{2(1+K)}{\exp(K) r_m^2} r \exp\left(-(1+K)\left(\frac{r}{r_m}\right)^2\right) \\ & \times I_0\left(2\sqrt{K(1+K)}\left(\frac{r}{r_m}\right)\right) \quad r \geq 0, \end{aligned} \tag{11}$$

$$P_r(r) = 1 - Q_1\left(\sqrt{2K}, \sqrt{2(1+K)}\left(\frac{r}{r_m}\right)\right) \quad r \geq 0. \tag{12}$$

The PDF and CDF in logarithmic units can be calculated as

$$\begin{aligned} p_{\varepsilon}(\varepsilon) = {} & \frac{2(1+K)}{A\exp(K)} \left(\frac{\exp\left(\frac{\varepsilon}{A}\right)}{r_m}\right)^2 \\ & \times \exp\left(-(1+K)\left(\frac{\exp\left(\frac{\varepsilon}{A}\right)}{r_m}\right)^2\right) \\ & \times I_0\left(2\sqrt{K(1+K)}\left(\frac{\exp\left(\frac{\varepsilon}{A}\right)}{r_m}\right)\right) \\ & -\infty < \varepsilon < \infty, \end{aligned} \tag{13}$$

$$\begin{aligned} P_{\varepsilon}(\varepsilon) = {} & 1 - Q_1\left(\sqrt{2K}, \sqrt{2(1+K)}\left(\frac{\exp\left(\frac{\varepsilon}{A}\right)}{r_m}\right)\right) \\ & -\infty < \varepsilon < \infty. \end{aligned} \tag{14}$$

C. FN

The parameter μ can be extended to natural numbers [10], [11]. If $\mu = 1/2$, r follows the FN distribution [33]. In this case, for convenience $\kappa_f = \kappa$. From [34] the modified Bessel function of the first kind with order $-1/2$ can be written as

$$I_{-\frac{1}{2}}(z) = \sqrt{\frac{2}{\pi}} \frac{\cosh(z)}{\sqrt{z}}. \tag{15}$$

Substituting $\mu = 1/2$ in (3) and using (15), the PDF of r can be expressed as [33]

$$\begin{aligned} p_r(r) = {} & \sqrt{\frac{2}{\pi}} \frac{\sqrt{1+\kappa_f}}{r_m} \exp\left(-\frac{\kappa_f}{2} - \frac{(1+\kappa_f)}{2}\left(\frac{r}{r_m}\right)^2\right) \\ & \times \cosh\left(\sqrt{\kappa_f(1+\kappa_f)}\left(\frac{r}{r_m}\right)\right) \quad r \geq 0, \end{aligned} \tag{16}$$

or alternatively

$$p_r(r) = \frac{1}{\sqrt{2\pi}s}\exp\left(-\frac{(r-\eta)^2}{2s^2}\right) + \frac{1}{\sqrt{2\pi}s}\exp\left(-\frac{(r+\eta)^2}{2s^2}\right) \quad r \geq 0, \quad (17)$$

where

$$\eta = \sqrt{\frac{\kappa_f}{1+\kappa_f}}r_m, \quad (18)$$

$$s = \sqrt{\frac{1}{1+\kappa_f}}r_m. \quad (19)$$

The CDF of r is given by [33]

$$P_r(r) = \Phi\left(\frac{r-\eta}{s}\right) + \Phi\left(\frac{r+\eta}{s}\right) = \frac{1}{2}\left(\operatorname{erf}\left(\frac{r-\eta}{\sqrt{2s^2}}\right) + \operatorname{erf}\left(\frac{r+\eta}{\sqrt{2s^2}}\right)\right) \quad r \geq 0, \quad (20)$$

where $\Phi(u) = \int_{-\infty}^{u}\frac{1}{\sqrt{2\pi}}\exp\left(-\frac{t^2}{2}\right)dt$ is the CDF of the standard normal distribution and $\operatorname{erf}(u) = \int_0^u \frac{2}{\sqrt{\pi}}\exp\left(-t^2\right)dt$ is the error function.

The PDF and CDF in logarithmic units are given by

$$p_\varepsilon(\varepsilon) = \sqrt{\frac{2}{\pi}}\frac{\sqrt{1+\kappa_f}}{Ar_m} \times \exp\left(-\frac{\kappa_f}{2} - \frac{(1+\kappa_f)}{2}\left(\frac{\exp\left(\frac{\varepsilon}{A}\right)}{r_m}\right)^2 + \frac{\varepsilon}{A}\right) \times \cosh\left(\sqrt{\kappa_f(1+\kappa_f)}\left(\frac{\exp\left(\frac{\varepsilon}{A}\right)}{r_m}\right)\right) \quad -\infty < \varepsilon < \infty, \quad (21)$$

$$P_\varepsilon(\varepsilon) = \Phi\left(\frac{\exp\left(\frac{\varepsilon}{A}\right)-\eta}{s}\right) + \Phi\left(\frac{\exp\left(\frac{\varepsilon}{A}\right)+\eta}{s}\right) = \frac{1}{2}\left(\operatorname{erf}\left(\frac{\exp\left(\frac{\varepsilon}{A}\right)-\eta}{s}\right) + \operatorname{erf}\left(\frac{\exp\left(\frac{\varepsilon}{A}\right)+\eta}{s}\right)\right) \quad -\infty < \varepsilon < \infty. \quad (22)$$

III. THE FN DISTRIBUTION

Physically, the FN distribution applied to the small-scale fading modeling considers a signal composed by a dominant component with multipath contributions. The variation in the phase of the sum of all the contributions is negligible compared to the variation of its amplitude. This situation corresponds to a strong dominant component in terms of the rest of multipath contributions typically found in LOS conditions.

A. NON-CENTRAL MOMENTS, MEAN AND VARIANCE

The non-central moments of the FN distribution are given by [35]

$$E\left[r^k\right] = s^k\sum_{j=0}^{k}\binom{k}{j}\eta^{k-j}\left(\mathcal{F}_j(-\eta) + (-1)^{k-j}\mathcal{F}_j(\eta)\right), \quad (23)$$

where

$$\mathcal{F}_j(a) = \frac{1}{\sqrt{2\pi}}\int_a^\infty y^j\exp\left(-\frac{y^2}{2}\right)dy, \quad j = 0, 1, 2, \ldots \quad (24)$$

Note that $\mathcal{F}_0(a) = 1 - \Phi(a)$. We can use the following recursive relationship

$$\mathcal{F}_j(a) = \frac{a^{j-1}}{\sqrt{2\pi}}\exp\left(-\frac{a^2}{2}\right) + (j-1)\mathcal{F}_{j-2}(a), \quad j = 0, 1, 2, \ldots, \quad (25)$$

and the identities $\Phi(-a) = 1 - \Phi(a)$ and $\mathcal{F}_1(-a) = \mathcal{F}_1(a) = \exp\left(-a^2/2\right)/\sqrt{2\pi}$ to calculate the non-central moments. From (18), (19), (23) and (25), the mean and the variance of the distribution can be calculated, respectively, as [36]

$$E[r] = \sqrt{\frac{2}{\pi}}\sqrt{\frac{1}{1+\kappa_f}}\left(\exp\left(-\kappa_f\right) + \sqrt{\kappa_f}\left(1 - 2\Phi\left(-\sqrt{\kappa_f}\right)\right)\right)r_m, \quad (26)$$

$$\operatorname{var}[r] = r_m^2 - (E[r])^2. \quad (27)$$

B. MOMENT GENERATING FUNCTION

The moment generating function of the FN distribution whose PDF is given by [33] can be written as

$$\mathcal{M}_r(t) = \exp\left(\frac{r_m^2}{2(1+\kappa_f)}t^2\right)\left[\exp\left(\frac{r_m}{\sqrt{1+\kappa_f}}t\right) \times \left(1 - \Phi\left(-\sqrt{\kappa_f} - \frac{r_m}{\sqrt{1+\kappa_f}}t\right)\right) - \exp\left(-\frac{r_m}{\sqrt{1+\kappa_f}}t\right) \times \left(1 - \Phi\left(\sqrt{\kappa_f} - \frac{r_m}{\sqrt{1+\kappa_f}}t\right)\right)\right]. \quad (28)$$

C. RELATIONSHIP WITH OTHER DISTRIBUTIONS

The FN distribution includes as a particular case the half-normal distribution. For $\kappa = 0$, $\eta = 0$ and $s = r_m$ the FN distribution becomes the half-normal distribution with PDF given by

$$p_r(r) = \frac{\sqrt{2}}{\sqrt{\pi}r_m}\exp\left(-\frac{r^2}{2r_m^2}\right) \quad r \geq 0, \quad (29)$$

with $E[r] = \sqrt{\frac{2}{\pi}}r_m$, and $\operatorname{var}[r] = r_m^2\left(1 - \frac{2}{\pi}\right)$.

Similarly to [10, (14)], substituting $\mu = 1/2$ in (7) the multiplicative inverse of the normalized variance of the power

of the fading signal, which is usually defined as m, can be expressed in terms of the κ parameter of the FN distribution, κ_f, as follows

$$m = \frac{E\left[r^2\right]}{\text{var}\left[r^2\right]} = \frac{\left(1+\kappa_f\right)^2}{2\left(1+2\kappa_f\right)}. \tag{30}$$

Note that the m parameter corresponds as well to the m fading parameter in case of the Nakagami-m distribution. Note that $m \geq 1/2$ provided that $\kappa_f \geq 0$.

For a given m, from (30) the equivalence to the κ_f parameter can be expressed as

$$\kappa_f = 2m - 1 + \sqrt{2m\left(2m-1\right)}, \tag{31}$$

which leads to $\kappa_f \geq 0$ for $m \geq 1/2$.

A relationship between the κ_f parameter of the FN distribution and the κ parameter of the κ-μ distribution can be established by matching the inverse multiplicative normalized variances in both distributions. Hence, κ_f can be calculated as a function of κ as (32), as shown at the bottom of this page.

In case of $\mu < 1/2$, (32) is consistent ($\kappa_f \in \mathbb{R}$, $\kappa_f \geq 0$) for

$$\kappa \geq \frac{1-2\mu+\sqrt{1-2\mu}}{2\mu}. \tag{33}$$

Likewise, the inverse relationship between κ_f and κ can be written as (34), as shown at the bottom of this page. If $\mu > 1/2$ then (34) is valid ($\kappa \in \mathbb{R}$, $\kappa \geq 0$) for

$$\kappa_f \geq 2\mu - 1 + \sqrt{2\mu\left(2\mu-1\right)}. \tag{35}$$

Fig. 1 shows the PDF in logarithmic units for the Rician and the FN distributions given by (13) and (21), respectively, with $r_m = 1$. The Rician K-factors used in the curves are $K = 0, 3, 5$ and 10 dB which correspond to $\kappa_f = 5.77, 7.52, 9$ and 13.33 dB, respectively, applying (32) with $\kappa = K$ and $\mu = 1$. As the Rician K-factor grows the PDFs of the Rician and FN distributions are becoming more and more similar in a way that both PDFs are indistinguishable for $K = 10$ dB which corresponds to $\kappa_f = 13.33$ dB. That fact corroborates the accurate approximation of the FN distribution to the Rician model with a strong dominant component in terms of the rest of the multipath contributions.

IV. MEASUREMENTS DESCRIPTION

The measurements were carried out in a lab of the Universidad Politécnica de Cartagena, Spain, with dimensions $8 \times 4.8 \times 3.5$ meters. As it can be seen from a picture of the lab

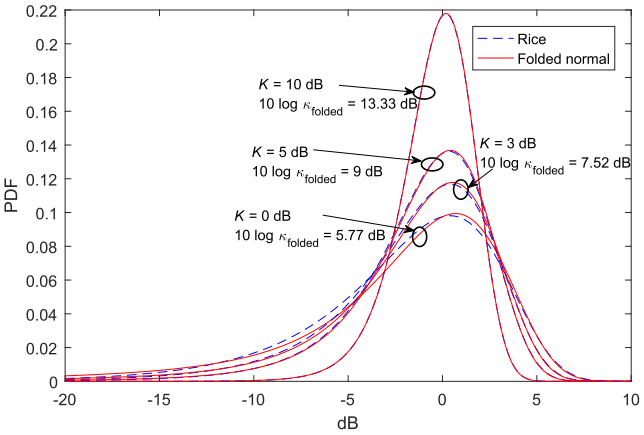

FIGURE 1. PDF of the Rician distribution and the equivalent folded normal distribution in logarithmic units for $r_m = 1$ and Rician K-factors $K = 0, 3, 5$ and 10 dB.

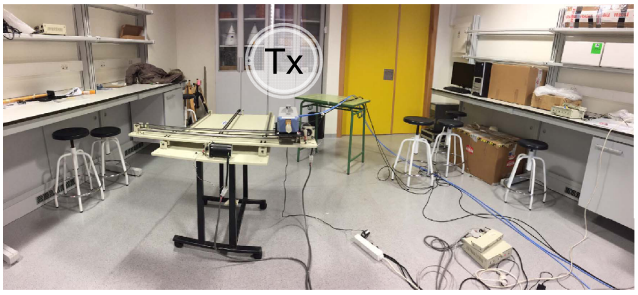

FIGURE 2. Lab with Tx antenna and positioner.

in Fig. 2, closets, desktops, chairs and shelves can be found as furniture. Four positions were established at the 60 GHz band and two positions at the 94 GHz band. Fig. 3 shows a map of the lab, with the distances from the Tx and Rx to the walls and the separation between Tx and Rx given by Table 1 for both the 60 and 94 GHz bands. The polarization was vertical for the Tx and vertical for the Rx (VV) at the 60 GHz band. At the 94 GHz band, two polarization combinations were used, either horizontal Tx and horizontal Rx (HH) or VV. The Tx and Rx antennas at both bands were located at a height of 0.784 and 0.886 m, respectively.

An R&S ZVA 67 vector network analyzer (VNA) and up-down converters were used as a channel sounder. Two identical omnidirectional antennas with linear polarization were used operating at both bands. At the 60 GHz band, Tx and Rx antennas manufactured by Steatite Q-Par provide the following relevant parameters: gain 5 dBi, BW 9 GHz,

$$\kappa_f = \frac{2\mu\kappa^2 + \left(4\mu-2\right)\kappa - 1 + 2\mu + \sqrt{2\mu\left(1+\kappa\right)^2\left(2\mu\kappa^2 + \left(4\mu-2\right)\kappa - 1 + 2\mu\right)}}{1+2\kappa} \tag{32}$$

$$\kappa = \frac{\kappa_f^2 + \left(2-4\mu\right)\kappa_f + 1 - 2\mu + \sqrt{\left(1+\kappa_f\right)^2\left(\kappa_f^2 + \left(2-4\mu\right)\kappa_f + 1 - 2\mu\right)}}{2\mu\left(1+2\kappa_f\right)} \tag{34}$$

TABLE 1. Position of the transmitter and receiver following the map of figure 3.

Frequency band	Position and polarization	A(m)	B(m)	C(m)	D(m)	Tx-Rx separation E(m)
60 GHz	1 VV	4.925	2.987	3.947	1.830	2.975
	2 VV	4.427	3.020	4.428	1.805	2.620
	3 VV	3.981	3.021	4.928	1.811	2.221
	4 VV	3.522	3.013	5.435	1.810	1.905
	Rx	1.940	1.523	5.712	3.308	-
94 GHz	1 HH	5.042	2.730	3.830	2.085	2.800
	2 VV	4.058	2.788	4.814	2.037	2.258
	Rx	1.667	1.620	5.985	3.220	-

TABLE 2. Parameters of measurements.

Frequency band	Position number	Polarization	Virtual array Tx	Virtual array Rx	Separation of the grid	Frequency points	Coherence bandwidth at 90%
60 GHz (57-66 GHz)	1	VV	ULA 1×20	ULA 1×20	0.25λ	2 048	1.606 MHz
	2	VV	ULA 1×20	ULA 1×20	0.25λ	2 048	1.621 MHz
	3	VV	ULA 1×20	ULA 1×20	0.25λ	2 048	2.620 MHz
	4	VV	ULA 1×20	ULA 1×20	0.25λ	2 048	3.111 MHz
94 GHz (92.5-95.5 GHz)	1	HH	URA 25×25	ULA 1×5	0.31λ	1 024	1.020 MHz
	2	VV	URA 25×25	ULA 1×5	0.28λ	1 024	2.193 MHz

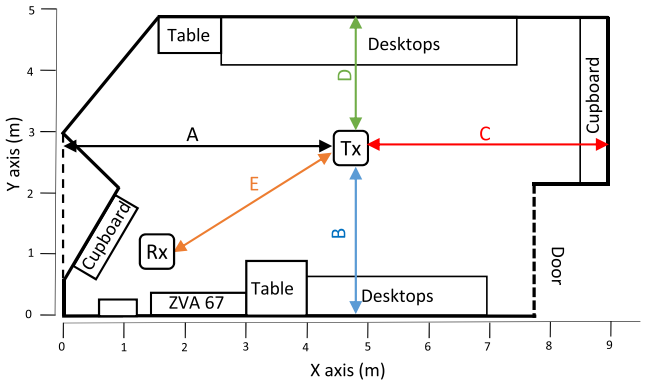

FIGURE 3. Map of the lab with distances corresponding to Table 1.

maximum voltage standing wave ratio (VSWR) 1.32 : 1, beamwidth in the E-plane 28° at 60 GHz and omnidirectional in the H-plane. The Tx and Rx antennas at the 94 GHz band were manufactured by Mi-Wave and have the next parameters: gain 2 dBi, BW 3 GHz, typical nominal VSWR 1.5 : 1, beamwidth in the E-plane 30° at 94 GHz and omnidirectional in the H-plane.

Table 2 shows the main parameters of the measurements. The Tx and Rx antennas were operated with Arrick Robotics positioners. Uniform linear arrays (ULA) and uniform rectangular arrays (URA) virtual systems were configured to obtain MIMO measurements. At the 60 GHz band, 20 elements were equally spaced along the Y-axis at both the Tx and Rx using ULA. At the 94 GHz band, for the URA Tx, measurements were performed over a 25×25 grid along the X and Y axes and for the ULA Rx, 5 elements were equally spaced along the Y-axis. The separation in the grid for both ULA Tx and ULA Rx was configured in 2 mm (0.25λ at 60 GHz) at the 60 GHz band. At the 94 GHz band, the grid separation was 1 mm (0.31λ at 94 GHz) and 0.89 mm (0.28λ at 94 GHz) for the positions 1 and 2, respectively. The number of points in frequency was chosen 2 048 at the 60 GHz band and 1 024 at the 94 GHz band. A BW of 10 Hz for the intermediate frequency filter was selected for both bands. The dynamic range obtained was approximately 110 and 107 dB without the effect of the antennas for the bands of 60 and 94 GHz, respectively. The measurements were carried out in stationarity conditions. More details about the parameters of the measurements can be consulted in [23] and [37] for the 60 and 94 GHz bands, respectively.

The coherence bandwidth calculated for an amplitude of the frequency autocorrelation function, R_T, of 0.9, ranges from 1.606 to 3.111 MHz at the 60 GHz band and was of 1.020 and 2.193 MHz for the location 1 and 2, respectively, at the 94 GHz band. The autocorrelation function was calculated from the Fourier transform of the power delay profile (PDP). The PDP was obtained by averaging the square amplitude of the channel impulse response over all the points in the grid.

V. DISTRIBUTION PARAMETER APPROXIMATION AND ESTIMATION

A. PARAMETER FITTING USING LEAST SQUARES METHOD

As a first approach, we have used the least squares (LS) method to find the parameters of all the analyzed distributions. This method is based on the minimization of the residual function given by

$$\min \left[\sum_{i=1}^{N} \left(P_{\exp}(\varepsilon_i) - \widehat{P}_{\varepsilon}(\varepsilon_i) \right)^2 \right], \tag{36}$$

where $P_{\text{exp}}(\cdot)$ represents the experimental CDF in logarithmic units; $\widehat{P}_{\varepsilon}(\cdot)$ is the approximated CDF in logarithmic units for the κ-μ, Rician and FN distributions given by (9), (14) and (22), respectively; and N is the number of the points in the discretized CDFs uniformly distributed between the maximum and the minimum value of the experimental samples of the distribution.

B. PARAMETER INFERENCE USING ESTIMATORS

To analyze the best-fit distribution, maximum likelihood (ML) estimators have been employed to infer the parameters of the Rician and FN distributions. To the best of the authors' knowledge ML estimators for the κ-μ have not been derived yet. The function `mle` of Matlab® implements an ML general numerical method which computes the parameter estimates using an iterative maximization algorithm. Unfortunately, a poor choice of starting point can cause the function `mle` to converge to a local optimum which is not the global maximizer, or to fail to converge entirely [38]. Generally speaking, the higher number of unknown parameters in the distribution to estimate the larger likelihood to obtain poorer results when using not proper starting values. What is interesting, the results for the κ-μ distribution with the measured data using the `mle` function with a generic starting point provide lower accuracy than those calculated using the method of moments (MM) derived in [11]. Therefore, in this case the κ and μ parameters of the κ-μ distribution will be estimated following the MM as [11, (9), (12)]

$$\hat{\kappa} = \frac{1}{\frac{\sqrt{2}(\widehat{M}_4 - 1)}{\sqrt{2\widehat{M}_4^2 - \widehat{M}_4 - \widehat{M}_6}} - 2}, \tag{37}$$

$$\hat{\mu} = \frac{1}{\widehat{\text{var}}_2} \frac{1 + 2\hat{\kappa}}{\left(1 + \hat{\kappa}\right)^2}, \tag{38}$$

where

$$\widehat{M}_4 = \frac{1}{n} \sum_{j=1}^{n} \hat{\rho}_j^4, \tag{39}$$

$$\widehat{M}_6 = \frac{1}{n} \sum_{j=1}^{n} \hat{\rho}_j^6, \tag{40}$$

$$\widehat{\text{var}}_2 = \frac{1}{n} \sum_{j=1}^{n} \hat{\rho}_j^4 - \left(\frac{1}{n} \sum_{j=1}^{n} \hat{\rho}_j^2 \right)^2. \tag{41}$$

$\widehat{M}_4$ and $\widehat{M}_6$ are the sample non-central moments or 4-th and 6-th order of $\rho = r/\hat{r}_m$, respectively, being $\hat{r}_m$ the sample r.m.s. given by

$$\hat{r}_m = \frac{1}{n} \sqrt{\sum_{j=1}^{n} \hat{r}_j^2}; \tag{42}$$

$\widehat{\text{var}}_2$ is the sample variance of $\rho^2 = \left(r/\hat{r_m}\right)^2$; n is the number of samples of the distribution; and ρ_j is the j-th sample of the distribution of ρ. Note that $\hat{\mu}$ calculated from (38) leads to a positive real number not necessarily integer provided that $\hat{\kappa} \geq 0$. This dissimilarity with the proposed theoretical model where μ is assumed integer can be explained by the fact that (1) is an approximate solution to the so-called random phase problem [10].

The K-factor of the Rician distribution can be estimated by solving for the root of the following equation [39]

$$\frac{1}{1 + \hat{K}} + \frac{1 + 2\hat{K}}{n\sqrt{\hat{K}\left(1 + \hat{K}\right)}} \sum_{j=1}^{n} \frac{\rho_j I_1\left(2\rho_j \sqrt{\rho_j\left(1 + \rho_j\right)}\right)}{I_0\left(2\rho_j \sqrt{\rho_j\left(1 + \rho_j\right)}\right)} = 1 + \frac{1}{n} \sum_{j=1}^{n} \rho_j^2, \tag{43}$$

where K is the estimated Rician K-factor.

In the case of the FN distribution, the log-likelihood estimators lead to the following equations [36]

$$\hat{s} = \sqrt{\hat{r}_m^2 - \hat{\eta}}, \tag{44}$$

$$\sum_{j=1}^{n} \frac{r_j}{1 + \exp\left(\frac{2\hat{\eta} r_j}{\hat{s}^2}\right)} = \frac{\sum_{j=1}^{n} \left(r_j - \hat{\eta}\right)}{2}, \tag{45}$$

where $\hat{\eta}$ and $\hat{s}$ are the estimated parameters of the FN distribution, given by (18) and (19), respectively. Using a recursive method, we can find a solution for $\hat{\eta}$ and $\hat{s}$ with (44) and (45), respectively. From (18) and (19) we can easily obtain an estimation of the κ_f parameter in the FN distribution as

$$\hat{\kappa}_f = \frac{\hat{\eta}^2}{\hat{s}^2}. \tag{46}$$

VI. RESULTS

First of all, the mean and the coefficient of variation of the fading distribution parameters for the Rician, FN, and κ-μ distributions are analyzed using the LS approximation. The coefficient of variation of a random variable is defined as the ratio of the sample standard deviation to the sample mean of a distribution and it provides an estimation of the variable dispersion [40]. Moreover, an assessment of the goodness-of-fit with the Kolmogorov-Smirnov (K-S) test and the best-fit distribution are analyzed for the LS approximation.

Next, an analysis of the goodness-of-fit with the K-S test and the best-fit distribution is carried out by inferring ML estimators for both the Rician and FN distributions and MM estimators for κ-μ distributions. It is worth noting that 2 048 distributions and 1 024 distributions at the 60 and 94 GHz bands, respectively, have been approximated and estimated in each one of the positions corresponding to each frequency sample. Each distribution comprises $n = 20 \times 20 = 400$ samples and $n = 5 \times 25 \times 25 = 3\,125$ samples for the 60 and 94 GHz bands, respectively. Hence a total of 8 192 distributions of 400 samples and 2 048 distributions of 3 125 samples were analyzed at the 60 and 94 GHz bands, respectively.

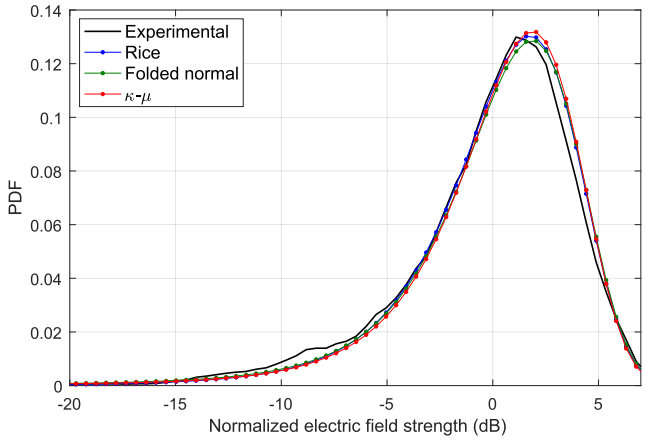

FIGURE 4. PDF of the normalized electric field strength for the experimental, and the approximated Rician, folded normal and κ-μ distributions in logarithmic units in the position 2 at the frequency of 92.5645 GHz with the VV polarization combination.

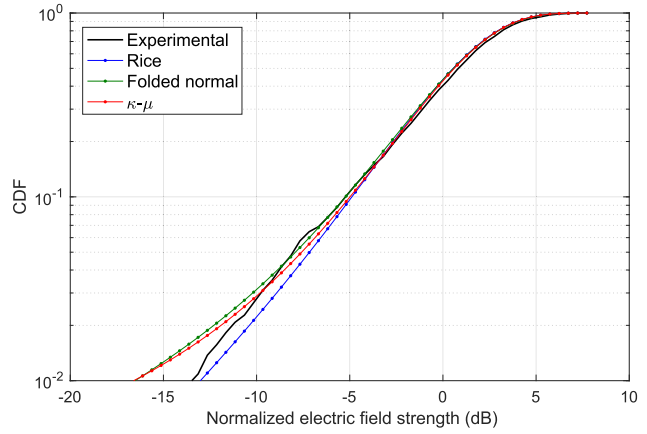

FIGURE 5. CDF of the normalized electric field strength for the experimental, and the approximated Rician, folded normal and κ-μ distributions in logarithmic units in the position 2 at the frequency of 92.5645 GHz with the VV polarization combination.

A. FADING DISTRIBUTION PARAMETERS

Using (36), we have calculated the approximated Rician, FN and κ-μ distribution parameters for each frequency sample in each measurement using LS with $N = 100$.

Fig. 4 shows an example of the PDF of the normalized field strength for the experimental, the approximated Rician, FN and κ-μ distributions in logarithmic units in the position 2 corresponding to the frequency of 92.5645 GHz with the VV polarization combination. There are very slight differences among the approximated Rician, FN and κ-μ distributions in this case. In Fig. 5 the CDF of the normalized field strength for the experimental, and the approximated Rician, FN and κ-μ distributions in logarithmic units with the same parameters of the Fig. 4 in order to illustrate the difference among such distributions and their approximation to the experimental distribution. The difference among such distributions is mainly perceived for values of the CDF lower than 10^{-1}. The κ-μ and FN CDFs tend to overlap for CDF values smaller than 10^{-2} in this case. Table 4 shows the mean and the coefficient of variation of the K parameter for the

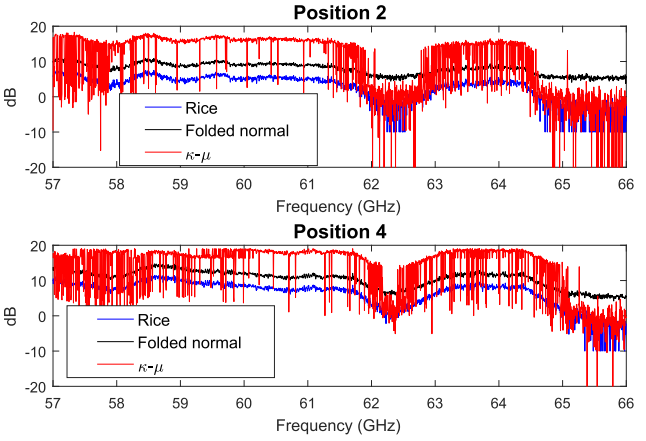

FIGURE 6. K-factor of the Rician, κ_f of the folded normal, and κ of the κ-μ distribution in logarithmic units as a function of the frequency using the LS approximation for the positions 2 and 4 at the 60 GHz band.

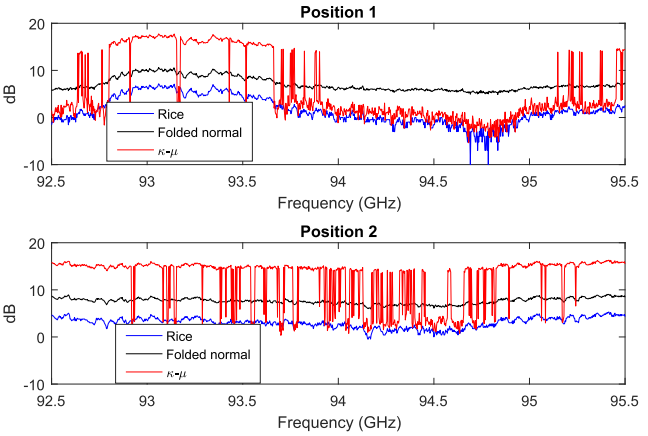

FIGURE 7. K-factor of the Rician, κ_f of the folded normal, and κ of the κ-μ distribution in logarithmic units as a function of the frequency using the LS approximation for the positions 1 and 2 at the 94 GHz band.

Rician distribution, κ_f for the FN distribution, and κ and μ for the κ-μ distribution. μ is expressed in linear units and K, κ_f and κ are calculated in dB.

It is worth noting that the less coefficient of variation calculated along the frequency the more stable is this parameter. The κ parameter of the κ-μ distribution and the Rician K-factor are significantly changeable along the frequency except for the position 2 with polarization VV at the 94 GHz band, provided that the coefficient of variation for the rest of positions of both bands ranges from 0.65 to 2.08 dB and from 0.54 to 1.18 dB for the Rician and for the κ-μ distributions, respectively. However, the coefficient of variation of the κ_f parameter for the FN distributions is substantially small, remaining under 0.26 dB and under 0.21 dB for the 60 and 94 GHz bands, respectively.

The mean of the μ parameter for the κ-μ distribution is 0.44 and 0.47 for the bands of 60 and 94 GHz, respectively. Since both values are significantly close to 0.5 the FN distribution could approximate and estimate accurately the experimental distribution in both bands in this environment.

Fig. 6 and 7 show the K-factor of the Rician, κ_f of the FN, and κ of the κ-μ distribution in logarithmic units in terms

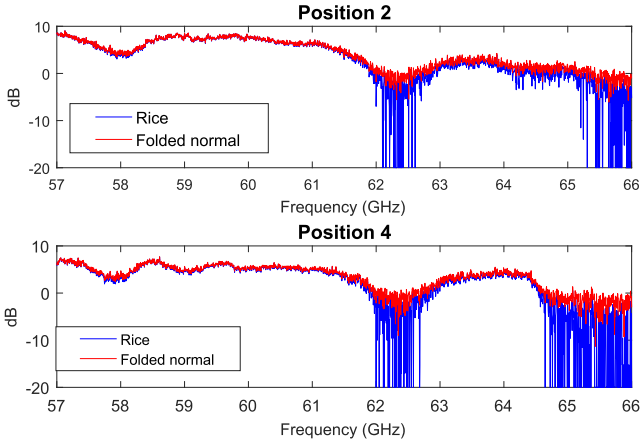

FIGURE 8. *K*-factor of the Rician distribution and equivalent *K*-factor of the folded normal distribution in logarithmic units as a function of the frequency using ML estimators for the positions 2 and 4 at the 60 GHz band.

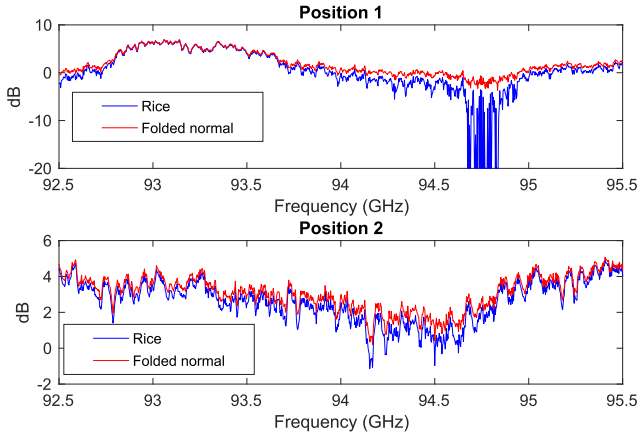

FIGURE 9. *K*-factor of the Rician distribution and equivalent *K*-factor of the folded normal distribution in logarithmic units as a function of the frequency using ML estimators for the positions 1 and 2 at the 94 GHz band.

of the frequency with the LS approximation for the 60 and 94 GHz bands, respectively. In Fig. 6 the position 2 and 4 were chosen whereas the position 1 and 2 were selected in Fig. 7. In each frequency bin, κ of the κ-μ distribution tends to the Rician K-factor or κ_f of the FN distribution depending on the value of the μ parameter found. Thus, if the approximated μ parameter is in the vicinity of 0.5, the approximated κ parameter tends to κ_f of the FN distribution. On the other hand, in case of the approximated μ parameter close to 1, the approximated κ parameter of the FN distribution can be approximated to the K-factor of the Rician distribution. The variation of the κ parameter in terms of the frequency is substantial particularly for the 60 GHz band and the position 2 of the 94 GHz band.

In Fig. 8 and 9, the estimated K-factor of the Rician distribution along with the equivalent K-factor of the FN distribution in dB are plotted as a function of the frequency with the ML estimators. The equivalent K-factor of the FN distribution has been calculated by substituting the estimated κ_f parameter in (34) with $\mu = 1$. At both bands the estimated K-factor of the Rician and the equivalent K-factor of the FN match substantially, except for the following ranges of frequencies: from 62.13 to 62.44 GHz and from 64.98 to 66 GHz in the position 2 at the band of 60 GHz, from 61.84 to 62.96 GHz and from 64.54 to 66 GHz in the position 4 at the band of 60 GHz and from 94.66 to 94.87 GHz in the position 1 at the 94 GHz band, where the K-factor of the Rician distribution experiments significant variations. In case of removing the values of such frequency ranges, the r.m.s. of the difference between the estimated K-factor of the Rician distribution and the equivalent K-factor of the FN distribution in dB is 0.31 and 0.22 dB for the positions 2 and 4 of the 60 GHz band, respectively, and 1.31 and 0.52 dB for the positions 1 and 2 of the 94 GHz band, respectively. Besides, it can be shown that the estimated K-factor of the Rician distribution remains under the equivalent K-factor of the FN distribution in all cases.

B. K-S TEST USING LS APPROXIMATION

To analyze the goodness-of-fit of the LS approximation and the ML and MM estimators, the K-S test can be used. The K-S test in one given frequency bin is fulfilled if the maximum absolute value between the experimental and the estimated CDFs, D_{est}, is lower or equal than a given value, $k_n(p)$, which depends on both the number of samples, n, and the significance level, p. Therefore, the condition to be accomplished in each frequency bin is as follows

$$D_{\text{est}} = \max_{j=1,\ldots,N} \left| P_{\text{exp}}(\varepsilon_i) - \widehat{P}_{\varepsilon}(\varepsilon_i) \right| \leq \delta_n(p), \qquad (47)$$

where $\delta_n(p) = B/\sqrt{n}$, being $B = 1.63$ and 1.36 for $p = 1\%$ and 5%, respectively; $P_{\text{exp}}(\cdot)$ is the experimental CDF in logarithmic units; $\widehat{P}_{\varepsilon}(\cdot)$ the estimated κ-μ, Rician or FN distribution CDF in logarithmic units given by (9), (14) and (22), respectively; and N is the number of the points in the discretized CDFs uniformly distributed between the maximum and the minimum value of the experimental samples of the distribution. In all the evaluations of the K-S test in this work, $N = 100$.

Table 3 shows the percentage of the best-fit distribution and the percentage of K-S fulfillment for a significance level of 1% for each position and for the whole measurement record at both bands using LS approximation. The percentage of the best-fit distribution has been calculated as the percentage of occurrence of the minimum value of D_{est} among the three analyzed distributions. It is worth noting that the sum of the best-fit percentages for each polarization combination and for all the measurement record is 100%. The maximum percentage of the best-fit distribution occurrence and the maximum percentage of the K-S test accomplishment have been highlighted in bold letters except for the K-S test fulfillment at the 60 GHz band because the percentages are equal or very close to 100% in this case. Since the LS is an approximation method and the κ-μ distribution is more general than the Rician and FN distribution including both of them as particular cases, the best-fit distribution and the

TABLE 3. Best-fit distribution percentages and K-S test fulfillment percentages with LS for a significance level of 1%.

Frequency band		Position	Polarization	Rician	Folded normal	$\kappa-\mu$
60 GHz	K-S 1%	1	VV	100	99.90	100
		2	VV	100	99.85	100
		3	VV	100	99.80	100
		4	VV	100	100	100
		All	VV	100	99.89	100
	Best-fit	1	VV	13.57	16.85	**69.58**
		2	VV	11.00	9.97	**79.03**
		3	VV	9.23	19.92	**70.85**
		4	VV	9.03	23.39	**67.58**
		All	VV	10.73	17.52	**71.75**
94 GHz	K-S 1%	1	HH	64.94	72.66	**78.52**
		2	VV	45.41	66.80	**81.54**
		All		55.18	69.73	**80.03**
	Best-fit	1	HH	16.91	29.91	**53.18**
		2	VV	4.78	15.92	**79.30**
		All		10.86	22.90	**66.24**

TABLE 4. Mean and coefficient of variation for the parameters calculated of the Rician, folded normal and $\kappa-\mu$ distributions using LS.

Frequency band	Position number and polarization	Rician K(dB)		Folded normal κ_f(dB)		$\kappa-\mu$ κ(dB)		μ	
		Mean	Coefficient of variation	Mean	Coefficient of variation	Mean	Coefficient of variation	Mean	Coefficient of variation
60 GHz	1 VV	3.44	1.12	8.46	**0.25**	9.85	0.83	0.50	1.03
	2 VV	2.46	1.67	7.92	**0.20**	9.62	0.89	0.44	1.06
	3 VV	5.32	0.74	9.76	**0.23**	12.59	0.62	0.41	1.29
	4 VV	6.27	0.65	10.51	**0.24**	13.30	0.54	0.43	1.33
	All	4.38	0.97	9.16	**0.26**	11.34	0.72	0.44	1.18
94 GHz	1 HH	1.43	2.08	7.07	**0.21**	6.04	1.18	0.65	0.59
	2 VV	3.02	0.37	7.62	**0.08**	12.21	0.42	0.29	1.15
	All	2.23	1.07	7.35	**0.16**	9.13	0.76	0.47	0.85

TABLE 5. Best-fit distribution percentages and K-S test fulfillment percentages for a significance level of 1% with ML estimators for both the Rician and folded normal distribution, and MM estimators for the κ-μ distribution.

Frequency band		Position	Polarization	Rician	Folded normal	$\kappa-\mu$
60 GHz	K-S 1%	1	VV	100	100	100
		2	VV	99.95	100	99.76
		3	VV	100	100	99.85
		4	VV	100	100	99.90
		All	VV	99.99	100	99.88
	Best-fit	1	VV	20.16	**53.08**	26.76
		2	VV	23.83	**50.54**	25.63
		3	VV	16.45	**59.28**	24.27
		4	VV	13.82	**62.89**	23.29
		All	VV	18.57	**56.44**	24.99
94 GHz	K-S 1%	1	HH	61.23	**72.85**	63.86
		2	VV	46.00	**66.80**	55.37
		All		53.61	**69.82**	59.62
	Best-fit	1	HH	16.99	**47.75**	35.25
		2	VV	8.59	**48.73**	42.68
		All		12.79	**48.24**	38.96

percentage of the accomplishment using the K-S test in the κ-μ distribution for a significance level of 1% is the highest among the three distributions analyzed.

Despite the fact that the mean of the Rician K-parameters at the 94 GHz band is not considerably high not exceeding 3.02 dB, the FN distribution provides K-S test fulfillment

percentages significantly close to those of the κ-μ distribution at this band. Moreover, the percentage of the best fitting is higher in the FN distribution than in the Rician distribution, except for the position 2 at the 60 GHz band. What is interesting, in spite of the fact that according to Table 4 the mean of the μ parameter in the four positions of the 60 GHz band is closer to 0.5 than the value obtained for the two positions of the 94 GHz band, the percentage of fulfillment using the K-S test for the FN distribution is higher at the 94 GHz than the 60 GHz band.

C. K-S TEST USING ESTIMATORS

The percentages of the best-fit distribution occurrence and the K-S test accomplishment for a significance of 1% are shown in Table 5 to assess the goodness-of-fit of the ML estimators for the Rician and FN distribution and MM estimators for the κ-μ distribution.

In this case the highest percentages of the best-fit distribution and the K-S test for a significance level of 1% correspond to the FN distribution. MM estimators in the κ-μ distribution involve both the 4th order and 6th order sample raw moments, thus the performance of these estimators given by (37) and (38) are not as accurate as those obtained with the LS approximation. Moreover, the percentages of K-S test fulfillment in both the Rician and the FN distribution with the ML estimators are similar to those calculated with the LS approximation.

VII. CONCLUSIONS

In this paper, a form of the FN distribution has been derived and applied to model the small-scale fading amplitude. This FN distribution is simple provided that it is biparametric, and does not involve complex functions in its PDF. Moreover, this distribution can be easily estimated through ML techniques following a recursive algorithm. The κ_f parameter of the FN distribution is also expressed as a function of an equivalent Rician K-factor, which is widely used in the literature. From a measurement campaign carried out in LOS condition in a lab, the FN distribution has been approximated by calculating the distribution parameters over frequency bins distributed in several locations for the Tx, where 8 192 and 2 048 distributions were analyzed at the 60 and 94 GHz bands, respectively. These approximated distribution parameters of the FN distribution have been compared to those obtained for the Rician and κ-μ distribution. Also, the parameters of these distributions have been estimated by using ML estimators for both the Rician and the FN distribution and MM estimators for the κ-μ distribution. The results of the K-S test show that the best-fit distribution among these three distributions is the FN distribution using ML estimators for both the Rician and the FN distribution and MM estimators for the κ-μ distribution in this LOS condition. Moreover, the approximated κ_f parameter of the FN distribution presents a smaller variation with the frequency than both the approximated κ parameter of the κ-μ distribution and the approximated Rician K-factor. Finally, the equivalent Rician K-factors calculated from the estimated κ_f parameters of the FN distribution show high similarity to the estimated Rician K-factors of the Rician distribution. Therefore, κ_f estimation of the FN distribution could be also useful to obtain more stable Rician K-factors from measurement records in LOS condition.

ACKNOWLEDGMENTS

The authors would like to thank the reviewers for their contributions to improve the final quality of this paper.

REFERENCES

[1] R. W. E. McNicol, "The fading of radio waves of medium and high frequencies," *Proc. IEE-Part III, Radio Commun. Eng.*, vol. 96, no. 44, pp. 517–524, Nov. 1949.

[2] E. Moore, "A unified approach to the detection of fluctuating pulsed signals in noise," *IEEE Trans. Inf. Theory*, vol. IT-13, no. 4, pp. 608–610, Oct. 1967.

[3] M. Nakagami, "The *m*-distribution—A general formula of intensity distribution of rapid fading," in *Statistical Methods in Radio Wave Propagation*, W. G. Hoffman, Ed. Oxford, U.K.: Pergamon Press, 1960, pp. 3–35.

[4] R. Ganesh and K. Pahlavan, "On the modeling of fading multipath indoor radio channels," in *Proc. IEEE Global Telecommun. Conf. Exhib. Commun. Technol. Beyond' (GLOBECOM)*, vol. 3, Nov. 1989, pp. 1346–1350.

[5] G. D. Durgin, T. S. Rappaport, and D. A. de Wolf, "New analytical models and probability density functions for fading in wireless communications," *IEEE Trans. Commun.*, vol. 50, no. 6, pp. 1005–1015, Jun. 2002.

[6] M. D. Yacoub, "The α-η-κ-μ fading model," *IEEE Trans. Antennas Propag.*, vol. 64, no. 8, pp. 3597–3610, Aug. 2016.

[7] G. Fraidenraich and M. D. Yacoub, "The α-η-μ and α-κ-μ fading distributions," in *Proc. IEEE 9th Int. Symp. Spread Spectr. Techn. Appl.*, Aug. 2006, pp. 16–20.

[8] M. D. Yacoub, "The α-μ distribution: A general fading distribution," in *Proc. 13th IEEE Int. Symp. Pers., Indoor Mobile Radio Commun.*, vol. 2, Sep. 2002, pp. 629–633.

[9] M. D. Yacoub, G. Fraidenraich, H. B. Tercius, and F. C. Martins, "The symmetrical η-κ distribution," in *Proc. IEEE 15th Int. Symp. Pers., Indoor Mobile Radio Commun.*, vol. 4, Sep. 2004, pp. 2426–2430.

[10] M. D. Yacoub, "The κ-μ distribution: A general fading distribution," in *Proc. IEEE 54th Veh. Technol. Conf. VTC Fall*, vol. 3, 2001, pp. 1427–1431.

[11] M. Yacoub, "The κ-μ distribution and the η-μ distribution," *IEEE Antennas Propag. Mag.*, vol. 49, no. 1, pp. 68–81, Feb. 2007.

[12] J. F. Paris, "Statistical characterization of κ-μ shadowed fading," *IEEE Trans. Veh. Technol.*, vol. 63, no. 2, pp. 518–526, Feb. 2014.

[13] L. Moreno-Pozas, F. J. Lopez-Martinez, J. F. Paris, and E. Martos-Naya, "The κ-μ shadowed fading model: Unifying the κ-μ and η-μ distributions," *IEEE Trans. Veh. Technol.*, vol. 65, no. 12, pp. 9630–9641, Dec. 2016.

[14] K. M. Mota, W. de Alvarenga Silva, U. S. Dias, and R. T. de Sousa Junior, "On the capacity analysis of κ-μ and α-μ fading channels for millimeter waves," in *Proc. SBMO/IEEE MTT-S Int. Microw. Optoelectron. Conf. (IMOC)*, Nov. 2015, pp. 1–5.

[15] E. Zöchmann, M. Hofer, M. Lerch, S. Pratschner, L. Bernadó, J. Blumenstein, S. Caban, S. Sangodoyin, H. Groll, T. Zemen, A. Prokeš, M. Rupp, A. F. Molisch, and C. F. Mecklenbräuker, "Position-specific statistics of 60 GHz vehicular channels during overtaking," *IEEE Access*, vol. 7, pp. 14216–14232, 2019.

[16] S. Rangan, T. S. Rappaport, and E. Erkip, "Millimeter-wave cellular wireless networks: Potentials and challenges," *Proc. IEEE*, vol. 102, no. 3, pp. 366–385, Mar. 2014.

[17] G. R. Maccartney, T. S. Rappaport, S. Sun, and S. Deng, "Indoor office wideband millimeter-wave propagation measurements and channel models at 28 and 73 GHz for ultra-dense 5G wireless networks," *IEEE Access*, vol. 3, pp. 2388–2424, 2015.

[18] S. Sun, T. S. Rappaport, M. Shafi, P. Tang, J. Zhang, and P. J. Smith, "Propagation models and performance evaluation for 5G millimeter-wave bands," *IEEE Trans. Veh. Technol.*, vol. 67, no. 9, pp. 8422–8439, Sep. 2018.

[19] S. Sun, T. S. Rappaport, T. A. Thomas, A. Ghosh, H. C. Nguyen, and I. Z. Kovács, I. Rodriguez, O. Koymen, and A. Partyka, "Investigation of prediction accuracy, sensitivity, and parameter stability of large-scale propagation path loss models for 5G wireless communications," *IEEE Trans. Veh. Technol.*, vol. 65, no. 5, pp. 2843–2860, May 2016.

[20] *IEEE Standard for Information Technology– Local and Metropolitan Area Networks– Specific Requirements– Part 15.3: Amendment 2: Millimeter-Wave-Based Alternative Physical Layer Extension*, IEEE Standard 802.15.3c-2009 (Amendment to IEEE Standard 802.15.3-2003), Oct. 2009, pp. 1–200.

[21] H. J. Thomas, R. S. Cole, and G. L. Siqueira, "An experimental study of the propagation of 55 GHz millimeter waves in an urban mobile radio environment," *IEEE Trans. Veh. Technol.*, vol. 43, no. 1, pp. 140–146, Feb. 1994.

[22] M.-S. Choi, G. Grosskopf, and D. Rohde, "Statistical characteristics of 60 GHz wideband indoor propagation channel," in *Proc. IEEE 16th Int. Symp. Pers., Indoor Mobile Radio Commun. (PIMRC)*, vol. 1, Sep. 2005, pp. 599–603.

[23] J. Reig, M.-T. Martínez-Inglés, L. Rubio, V. M. Rodrigo Peñarrocha, and J.-M. Molina-García-Pardo, "Fading evaluation in the 60 GHz band in line-of-sight conditions," *Int. J. Antennas Propag.*, vol. 2014, Aug. 2014, Art. no. 984102.

[24] S. K. Yoo, S. L. Cotton, R. W. Heath, and Y. J. Chun, "Measurements of the 60 GHz UE to eNB channel for small cell deployments," *IEEE Wireless Commun. Lett.*, vol. 6, no. 2, pp. 178–181, Apr. 2017.

[25] A. Kajiwara, "Indoor propagation measurements at 94 GHz," in *Proc. 6th Int. Symp. Pers., Indoor Mobile Radio Commun.*, vol. 3, Sep. 1995, pp. 1026–1030.

[26] J. Helminger, J. Detlefsen, and H. Groll, "Propagation properties of an indoor-channel at 94 GHz," in *Proc. Int. Conf. Microw. Millim. Wave Technol. (ICMMT)*, Aug. 1998, pp. 9–14.

[27] B. Hanssens, M.-T. Martínez-Inglés, E. Tanghe, D. Plets, J. M. Molina-García-Pardo, C. Oestges, L. Martens, and W. Joseph, "Measurement-based analysis of specular and dense multipath components at 94 GHz in an indoor environment," *IET Microw., Antennas Propag.*, vol. 12, no. 4, pp. 509–515, 2018.

[28] J. Reig, M. T. Martínez-Inglés, J. M. Molina-García-Pardo, L. Rubio, and V. M. Rodrigo-Peñarrocha, "Small-scale distributions in an indoor environment at 94 GHz," *Radio Sci.*, vol. 52, no. 7, pp. 852–861, Jul. 2017.

[29] C. Sanchis-Borrás, M. Martínez-Inglés, J. Molina-García-Pardo, J. P. García, and J. Rodríguez, "Experimental study of MIMO-OFDM transmissions at 94 GHz in indoor environments," *IEEE Access*, vol. 5, pp. 7488–7494, 2017.

[30] M. K. Simon and M.-S. Alouini, *Digital Communication Over Fading Channels*, 2nd ed. Hoboken, NJ, USA: Wiley, 2005.

[31] I. S. Gradshteyn and I. M. Ryzhik, *Table of Integrals, Series, and Products*, 7th ed. San Diego, CA, USA: Academic, 2007.

[32] J. Marcum, *Table Q Functions* (Memorandum). Santa Monica, CA, USA: Rand, 1950.

[33] F. S. Leone, L. S. Nelson, and R. B. Nottingham, "The folded normal distribution," *Technometrics*, vol. 3, no. 4, pp. 543–550, 1961.

[34] (Mar. 2019). *The Wolfram Functions Site. BesselI Function*. [Online]. Available: http://functions.wolfram.com/03.02.03.0005.01

[35] R. C. Elandt, "The folded normal distribution: Two methods of estimating parameters from moments," *Technometrics*, vol. 3, no. 4, pp. 551–562, 1961.

[36] M. Tsagrisa, C. Beneki, and H. Hassani, "On the folded normal distribution," *Mathematics*, vol. 2, no. 1, pp. 12–28, 2014.

[37] M.-T. Martínez-Inglés, D. P. Gaillot, J. Pascual-García, J.-M. Molina-García-Pardo, J.-V. Rodríguez, L. Rubio, and L. Juan-Llácer, "Channel sounding and indoor radio channel characteristics in the W-band," *EURASIP J. Wireless Commun. Netw.*, vol. 2016, no. 1, p. 30, Jan. 2016.

[38] (Mar. 2019) *Mle Function. Matlab R2018b. MathWorks*. [Online]. Available: https://www.mathworks.com/help/stats/mle.html

[39] K. K. Talukdar and W. D. Lawing, "Estimation of the parameters of the Rice distribution," *J. Acoust. Soc. Amer.*, vol. 89, no. 3, pp. 1193–1197, 1991.

[40] B. S. Everitt and A. Skrondal, *The Cambridge Dictionary of Statistics*, 4th ed. Cambridge, U.K.: Cambridge Univ. Press, 2010.

JUAN REIG received the Ph.D. degree from the Universitat Politècnica de València (UPV), Spain, in 2000. He has been a Faculty Member of the Department of Communications, UPV, since 1994, where he is currently a Full Professor of telecommunication engineering. He is a member of the Electromagnetic Radiation Group (GRE), Institute of Telecommunications and Multimedia Applications (iTEAM). His areas of interest include fading theory, diversity, ultra-wideband (UWB) systems, vehicular communications, and millimeter wave (mmWave) propagation.

VICENT MIQUEL RODRIGO PEÑARROCHA was born in Valencia, Spain, in 1966. He received the M.S. degree in telecommunications engineering from the Universidad Politécnica de Madrid, Spain, in 1990, and the Ph.D. degree in telecommunications engineering from the Universitat Politècnica de València, Spain, in 2003, where he joined the Departamento de Comunicaciones, in 1991, as a Lecturer. His current interests include radiowave propagation, antenna measurements, instrumentation, virtual instrumentation and laboratories, and any educational activity.

LORENZO RUBIO was born in El Ballestero, Albacete, Spain, in 1971. He received the M.S. and the Ph.D. degrees in telecommunications engineering from the Universitat Politècnica de València (UPV), Spain, in 1996 and 2004, respectively. In 1996, he joined the Communications Department, UPV, where he is currently a Full Professor of wireless communications. His main research interest includes wireless communications. His specific current research topics include radiowave propagation, measurement and mobile time-varying channels modeling in vehicular applications, ultra-wideband (UWB) communication systems, multiple-input multiple-output (MIMO) systems, and equalization techniques in digital wireless systems. He has received the Ericsson Mobile Communications Prize from the Spanish Telecommunications Engineer Association for his study on urban statistical radiochannels characterization applied to wireless communications.

MARÍA TERESA MARTÍNEZ-INGLÉS was born in Murcia, Spain, in 1983. She received the Telecommunications Engineering degree and the Ph.D. degree in telecommunications from the Universidad Politécnica de Cartagena (UPCT), Cartagena, Spain, in 2009 and 2014, respectively. In 2016, she joined the University Center of Defense, San Javier Air Force Base, MDE, UPCT, Murcia, Spain, where she is currently an Associate Professor. Her current research interest includes the modeling and the characterization of the millimeter-wave frequency bands.

JOSE MARÍA MOLINA-GARCÍA-PARDO received the degree in telecommunications engineering from the Universidad Politecnica de Valencia, in 2000, and the Ph.D. degree in telecommunications from the Universidad Politécnica de Cartagena, in 2004, where he has been an Associate Professor, since 2007, and a Full Professor, since 2016. He has authored over 70 journals articles indexed in the JCR and three book chapters. He has over 100 international conferences.. His research activities include radio communications, propagation, channel modeling, and experimental channel sounding for different frequency bands (300 MHz–400 GHz) and technologies, such as GSM, UMTS, LTE, WiFi, WSN, TETRA, mmW, OFDM, MIMO, BAN, and cognitive radios.